

Improved semiclassical dynamics through adiabatic switching trajectory sampling

Riccardo Conte,^{*} Lorenzo Parma, Chiara Aieta, Alessandro Rognoni, and Michele Ceotto[†]

Dipartimento di Chimica, Università degli Studi di Milano, via Golgi 19, 20133 Milano, Italy

Abstract

We introduce an improved semiclassical dynamics approach to quantum vibrational spectroscopy. In this method, a harmonic-based phase space sampling is preliminarily driven toward non-harmonic quantization by slowly switching on the actual potential. The new coordinates and momenta serve as initial conditions for the semiclassical dynamics calculation, leading to substantial decrease in the number of chaotic trajectories to deal with. Applications are presented for model and molecular systems of increasing dimensionality characterized by moderate or high chaoticity. They include a bidimensional Henon-Heiles potential, water, formaldehyde, and methane. The method improves accuracy and precision of semiclassical results and it can be easily interfaced with all pre-existing semiclassical theories.

^{*} riccardo.conte1@unimi.it

[†] michele.ceotto@unimi.it

I. INTRODUCTION

Chaotic systems can be found in several research fields ranging, for instance, from physics to meteorology, from chemistry to economy. They often constitute a hindrance to the possibility of making accurate predictions and a difficult challenge to face.

This is also the case for semiclassical (SC) dynamics, which has the peculiar feature of reproducing quantum effects accurately starting from classical trajectory runs.[1–13] This hallmark and the possibility to be employed straightforwardly with any fitted or “on-the-fly” potential energy surface (PES) make SC dynamics appealing for vibrational spectroscopy of complex molecules[14–17] as well as a reference for quantum spectroscopy of medium-large dimensional systems.[18–27]

The state-of-art is the result of several efforts in the advance of SC dynamics. A milestone in the development of SC vibrational spectroscopy is represented by Kaledin and Miller’s time-averaged semiclassical initial value representation (TA SCIVR),[28, 29] which has permitted to extend applicability of the coherent state semiclassical Herman Kluk propagator[30] to small molecules overcoming the well-known convergence issue of the Monte Carlo phase space integration.[31–33]

Applications to much larger systems are now possible thanks to the very recent divide-and-conquer semiclassical initial value representation technique (DC SCIVR), which is based on the projection of the full-dimensional investigation onto a set of lower dimensional targets.[34–36] It is useful to remark, though, that for the large systems studied by means of DC SCIVR a proper Monte Carlo convergence cannot be achieved, due to the computational overhead that such a computation would require. Thereby, the simulation must rely on a limited number of trajectories often evolved “on-the-fly” at some accessible *ab initio* level of electronic structure theory.

On this regard, pivotal work by De Leon and Heller has demonstrated that quantum eigenvalues can be calculated exactly by means of SC dynamics even employing a single trajectory, provided it has the correct (unknown) energy.[37] By further developing this idea, one of us has introduced the multiple coherent states semiclassical initial value representation (MC SCIVR), whereby accurate estimates for the quantum frequencies of vibration are obtained on the basis of a single or handful of trajectories.[38–41]

These methods restrict the original TA-SCIVR phase space sampling to a smaller region or even a single point, while the sampling is done in a harmonic fashion due to the availability of har-

monic estimates at low computational cost even for medium-large molecular systems. However, the harmonic approximation typically overestimates the true energy, sometimes even substantially. Furthermore, the actual potential is not harmonic and the initial harmonic state is not a stationary state of the molecular Hamiltonian. These aspects contribute to the numerical instability of the ensuing trajectories and deteriorate accuracy and precision of semiclassical results.

Adiabatic switching (AS) is a technique that may help overcome these issues. It has been developed to attain non-harmonic quantization and sample initial conditions in quasi-classical trajectory (QCT) simulations. Its foundation lies in the classical adiabatic theorem which states that action variables are constants of motion during the evolution of a trajectory lying on a phase-space torus not only for an isolated system but also in presence of a perturbation, provided that the latter is switched on very slowly (ideally over an infinite period of time). [42–47] AS has also been employed to obtain Wigner distributions[48, 49] and for estimates of vibrational energies.[50, 51] Qu and Bowman recently adopted AS to determine the zero-point energy (ZPE) and fundamental frequencies of a couple of modes of methane, showing the importance to perform adiabatic switching in an Eckart frame to get to a narrower and more accurate energy distribution.[52] Further improvements in precision and accuracy have been later provided by Nagy and Lendvay by developing AS in internal coordinates to prevent any kind of ro-vibrational coupling.[53] However, differently from several quantum methods and semiclassical approaches,[54, 55] adiabatic switching is not able to provide eigenfunctions. Furthermore, AS efficiency is expected to deteriorate for increasing values of the density of vibrational states, which is known to grow fast with energy.[56, 57]

To better point out the focus of this paper, we recall that n -dimensional integrable systems are those for which n independent integrals of motion satisfying the Poisson bracket condition can be found and quantization is doable because the integrals of motion correspond to commuting observables. In this case trajectories lie on the surface of tori in phase space. Such trajectories are stable, do not show any chaotic behavior and never fill up the whole phase space. Conversely, molecular systems are in general non integrable and trajectories eventually lead to numerical instability. The basic idea of this work is that adiabatic switching, starting from the separable and easily quantizable system made of n harmonic oscillators, can provide an approximate quantization, which, at least for the short times involved in a semiclassical spectroscopic calculation, allows use of more stable, quasi-periodic trajectories. Consequently, the main goal of this manuscript is to demonstrate that the AS technique allows one to sample the initial phase space conditions of

semiclassical simulations in a more effective way, decreasing substantially the number of chaotic, numerically unstable trajectories to deal with, and improving precision and accuracy of results. We label this “adiabatically switched” semiclassical approach as AS SCIVR.

In Section II we report on the theoretical and computational details of the method. Section III is dedicated to the application of AS SCIVR to a Henon-Heiles model potential and molecular systems of increasing dimensionality from water to methane. Finally, we summarize results and discuss possible future developments and applications of the method in Section IV.

II. THEORETICAL AND COMPUTATIONAL DETAILS

The basic semiclassical working formula we adopted for this paper is

$$I(E) = \frac{1}{(2\pi\hbar)^{N_{vib}}} \int d\mathbf{p}_0 \int d\mathbf{q}_0 \frac{1}{2\pi\hbar T} \left| \int_0^T dt' e^{i[S_{t'}(\mathbf{p}_0, \mathbf{q}_0) + \phi_{t'}(\mathbf{p}_0, \mathbf{q}_0) + Et']/\hbar} \langle g_{t'}(\mathbf{p}_0, \mathbf{q}_0) | \Psi \rangle \right|^2. \quad (1)$$

In Eq. (1) $I(E)$ is the energy-dependent density of vibrational states, whose peaks are located at the SC frequencies of vibration; N_{vib} is the number of vibrational degrees of freedom; T is the total simulation time; $S_{t'}$ is the instantaneous classical action calculated along the trajectory originated from the $(\mathbf{p}_0, \mathbf{q}_0)$ point in phase space, and $\langle g_{t'}(\mathbf{p}_0, \mathbf{q}_0) | \Psi \rangle$ is the quantum mechanical overlap between the coherent state basis element $|g_{t'}(\mathbf{p}_0, \mathbf{q}_0)\rangle$ and the reference state $|\Psi\rangle$. A coherent state with Gaussian width matrix Γ is defined as

$$\langle \mathbf{q} | g_{t'}(\mathbf{p}_0, \mathbf{q}_0) \rangle = \left(\frac{\det(\Gamma)}{\pi^{N_{vib}}} \right)^{1/4} \exp \left[-(\mathbf{q} - \mathbf{q}_{t'})^T \frac{\Gamma}{2} (\mathbf{q} - \mathbf{q}_{t'}) + \frac{i}{\hbar} \mathbf{p}_{t'}^T (\mathbf{q} - \mathbf{q}_{t'}) \right], \quad (2)$$

where $\mathbf{p}_{t'}$ and $\mathbf{q}_{t'}$ are the momentum and position vectors at time t' obtained upon classical Hamiltonian evolution from $(\mathbf{p}_0, \mathbf{q}_0)$. Γ is usually chosen to be a diagonal matrix with elements equal to the harmonic frequencies of vibration. For the calculations presented here we employed reference states $|\Psi\rangle$ made of suitable combinations of coherent states centered at equilibrium coordinates and harmonically estimated momenta, in agreement with our previous works.[58] Finally, $\phi_{t'}$ is the phase of the so-called Herman-Kluk prefactor

$$\phi_{t'}(\mathbf{p}_0, \mathbf{q}_0) = phase \left[\sqrt{\left| \frac{1}{2} \left(\frac{\partial \mathbf{q}_{t'}}{\partial \mathbf{q}_0} + \Gamma^{-1} \frac{\partial \mathbf{p}_{t'}}{\partial \mathbf{p}_0} \Gamma - i\hbar \frac{\partial \mathbf{q}_{t'}}{\partial \mathbf{p}_0} \Gamma + \frac{i\Gamma^{-1}}{\hbar} \frac{\partial \mathbf{p}_{t'}}{\partial \mathbf{q}_0} \right) \right|} \right]. \quad (3)$$

The prefactor is related to deterministic chaos through the monodromy matrix elements $(\partial \mathbf{i} / \partial \mathbf{j})$ $\mathbf{i} = \mathbf{p}_{t'}, \mathbf{q}_{t'}$; $\mathbf{j} = \mathbf{p}_0, \mathbf{q}_0$). In fact, when one or more of the monodromy matrix eigenvalues start to grow exponentially in the chaotic regime, numerical integration of the Herman-Kluk prefactor becomes more and more inaccurate and, eventually, an unphysical divergence is reached spoiling the entire SC calculation. Several approaches have been employed to overcome this issue. The basic one consists in completely discarding trajectories that reveal a chaotic behavior at some point during the dynamics. As an alternative, it has been proposed to keep trajectories up to the instant when numerical instability kicks in, possibly by weighing their contributions appropriately.[16, 59] A different way to tackle the problem is by approximating or regularizing the prefactor.[60–63] However, none of these approaches is able to provide a way to restrict the semiclassical calculation to non-chaotic trajectories beforehand.

The other technique employed in this work is adiabatic switching. The AS procedure involves definition of a separable vibrational Hamiltonian (H_0) for which quantization is known or easily achieved, followed by introduction of the true molecular potential at slow pace until the fully-coupled vibrational molecular Hamiltonian (H) is reached. In practice, upon calculation of the set of harmonic frequencies of vibration $\{\omega_i\}$, H_0 is generally chosen to be the harmonic approximation to H in mass scaled coordinates and momenta

$$H_0 = \sum_{i=1}^{N_{vib}} \left(\frac{p_i^2}{2} + \frac{\omega_i^2 q_i^2}{2} \right), \quad (4)$$

and the AS Hamiltonian (H^{AS}) is a function of time

$$H^{AS}(t) = H_0 + f_S(t)(H - H_0). \quad (5)$$

$f_S(t)$ is a switching function selected in agreement with the literature[52]

$$f_S(t) = \frac{t}{T_{AS}} - \frac{1}{2\pi} \sin \left(\frac{2\pi t}{T_{AS}} \right), \quad (6)$$

which equals 0 at $t = 0$ and 1 at $t = T_{AS}$, the total AS simulation time. For the harmonic Hamiltonian, initial normal mode coordinates and momenta can be obtained straightforwardly from action-angle variables, i.e. $q_i = [(2n_i + 1)\hbar/\omega_i]^{1/2} \cos \zeta_i$; $p_i = -[(2n_i + 1)\hbar\omega_i]^{1/2} \sin \zeta_i$. n_i are integer actions, while ζ_i are randomly selected angles from a uniform distribution. Classical dynamics is then performed for a time T_{AS} under the Hamiltonian $H^{AS}(t)$. Clearly, during adiabatic switching, the total energy is not conserved. It starts from the harmonic value and ends at an

estimate of the energy of the corresponding quantized state of the actual molecular Hamiltonian. From an ensemble of AS trajectories, one eventually gets a distribution that approximates the energy of the state, as shown for methane in Figure 1. We employed a pre-existing methane PES by Lee, Martin and Taylor.[64] T_{AS} was chosen equal to 1.21 ps (50000 atomic units), a time step of 0.242 fs was employed, and the dynamics, as for all other investigations presented in this paper, was integrated by means of a 4-th order symplectic algorithm with a fixed step equal to 10^{-3} for finite difference calculations.[65]

Because adiabatic switching is known to work more efficiently at low density of vibrational states and for not strongly coupled systems,[51] we employed it to get an initial distribution in phase space for our subsequent and more widely applicable semiclassical dynamics simulations. In other words, the outcome of the adiabatic switching procedure served as an initial sampling for the SCIVR spectral calculations. We evolved the dynamics in normal modes in agreement with our past standard TA-SCIVR applications. Fig. 2 shows a comparison for methane between the AS final energy distributions of 9000 trajectories obtained starting from harmonic ZPE sampling by means of the approach reported in Ref. 52 and our normal-mode based one. Computational details are the same as previously reported. Results are in strict agreement. We removed the rovibrational coupling in our normal mode reference frame by not evolving the rotational degrees of freedom, an artefact which, on the other hand, slightly perturbs the total angular momentum, owing to the loss of reliability of normal modes out of equilibrium. This led to the very small (but negligible for our purposes) discrepancy between the two simulations. For the Gaussian envelop of bins a width of 7.2 cm^{-1} has been adopted in all simulations.

As for TA SCIVR and the semiclassical part of our AS-SCIVR simulations, to determine whether a classical trajectory had to be discarded or not, we compared along the dynamics the shift from unity of the monodromy matrix determinant to an arbitrary threshold σ . [28, 66] Whenever the shift was larger than the chosen σ we eliminated the whole trajectory from the set of those contributing to the final spectrum.

III. RESULTS

To demonstrate the performance of AS SCIVR we applied it to a set of systems, characterized by different regimes of trajectory rejection, and compared the outcomes with the corresponding ones obtained by using a standard TA-SCIVR procedure. Results were also tested against available

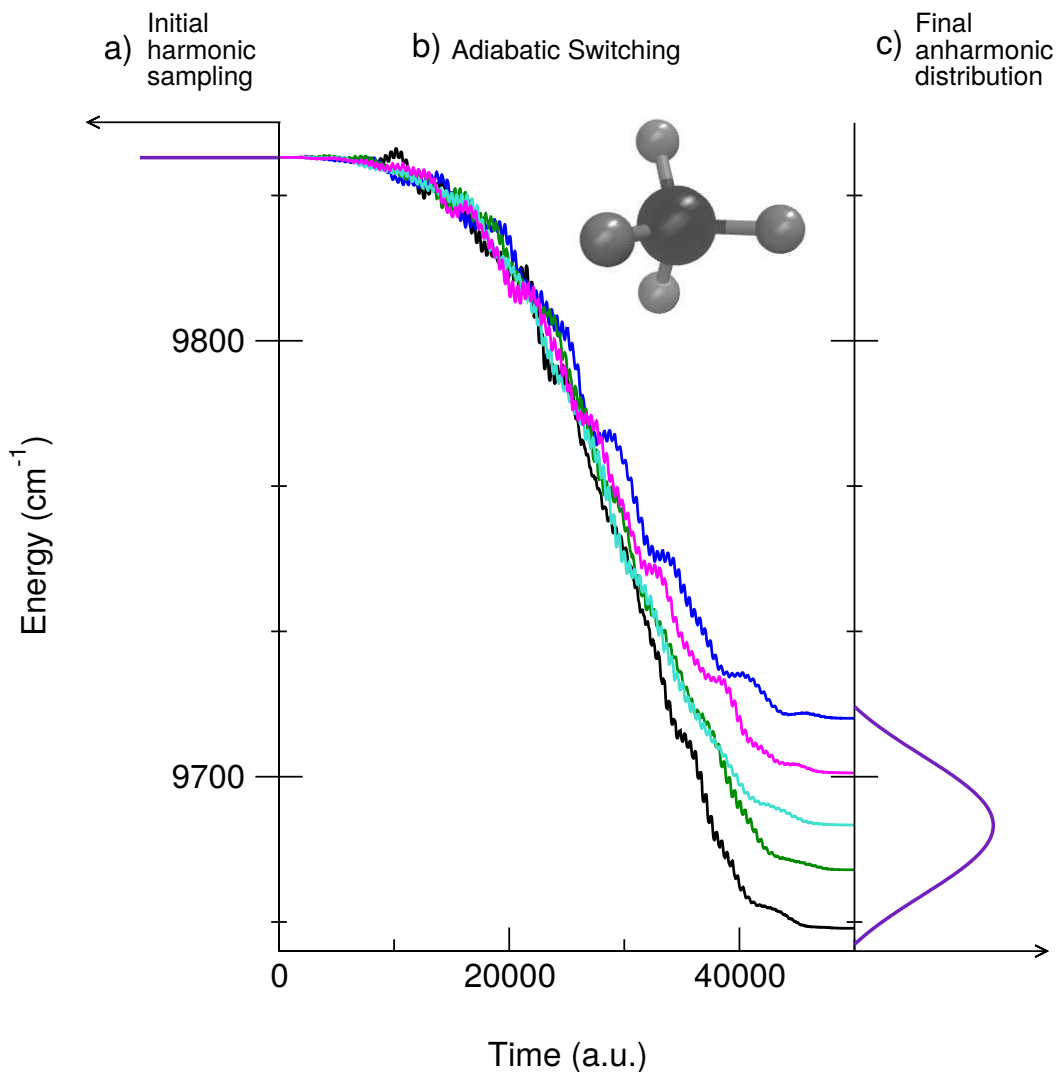


Figure 1. Representation of the adiabatic switching procedure for methane. Panel a): Trajectories are given the harmonic ZPE energy (violet). Panel b): The energy of 5 trajectories (different colors) is reported as they evolve under the adiabatic switching Hamiltonian. Panel c): A final distribution of anharmonic energies (violet) is found.

quantum mechanical benchmarks.

A. Henon-Heiles model

We start presenting an application to a low-dimensional model system characterized by moderate chaos. We chose the following two-dimensional Henon-Heiles potential, which was employed also in previous works[4, 67, 68]

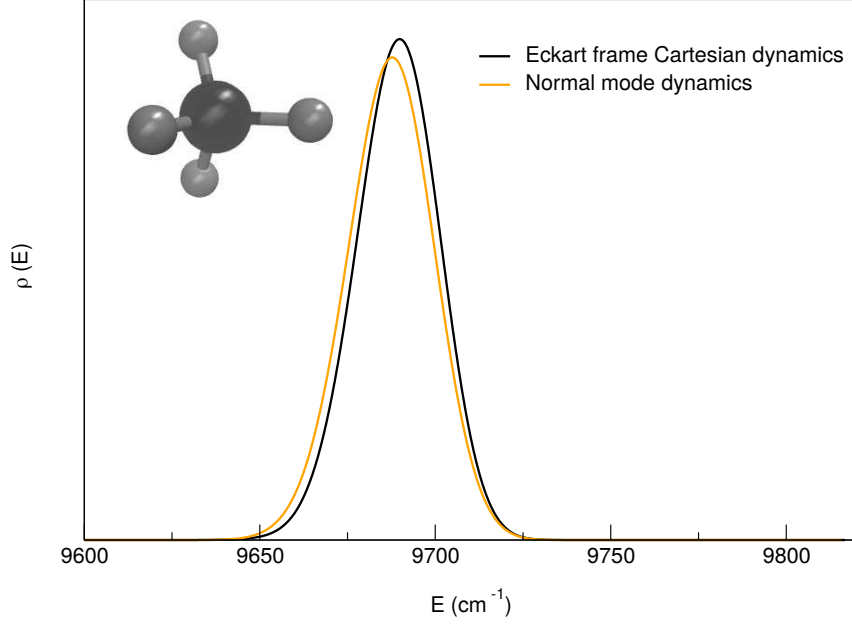


Figure 2. Final AS energy distributions for methane started with harmonic zero point energy (9842 cm^{-1}). Comparison is between Cartesian dynamics in Eckart frame (maroon), as described in Ref. 52, and the normal mode dynamics employed in this work (orange).

$$V(q_1, q_2) = \frac{1}{2}\omega_1^2 q_1^2 + \frac{1}{2}\omega_2^2 q_2^2 + \lambda q_2(q_1^2 + \eta q_2^2) \quad \omega_1 = 1.3, \omega_2 = 0.7, \lambda = -0.1, \eta = 0.1. \quad (7)$$

Values of the parameters in Eq. (7) are given in atomic units (a.u.). This leads to a different time scale for the dynamics with respect to the case of methane. In particular, T_{AS} was set to 12.1 fs and T was selected equal to about 121 fs with a timestep of 0.00242 fs. A different SC calculation for each of the first 8 eigenvalues was performed by means of both AS SCIVR and TA SCIVR. Initial conditions were determined either by centering a Husimi distribution at the harmonic energy of the target eigenvalue (TA-SCIVR simulations), or by starting a preliminary AS procedure from the relevant harmonic quantization (AS-SCIVR simulations). TA SCIVR featured a trajectory rejection rate ranging from about 36% to 79% given a threshold $\sigma = 10^{-6}$. Under the same strict condition, all trajectories generated for AS-SCIVR simulations were instead suitable to be employed. Table I shows a comparison of the first 8 eigenvalues obtained by means of the discrete variable representation method (DVR), TA SCIVR, and AS SCIVR. For the sinc-DVR calculation[69] we employed a rectangular grid ([-5:5], [-8:8]) with 70 points per each dimension without any energy cutoff. Both semiclassical simulations provide results in perfect agreement

Table I. Calculated eigenvalues and full widths at half maximum (in parenthesis) for the first 8 energy levels of a 2-dimensional Henon Heiles model. Values are in atomic units. Under the column for Level the corresponding harmonic excitation is given in parenthesis.

Level	DVR	TA SCIVR	AS SCIVR
0 (ZPE)	0.996	0.996 (0.002)	0.996 (0.001)
1 (ω_2)	1.687	1.687 (0.003)	1.687 (0.001)
2 (ω_1)	2.278	2.278 (0.003)	2.278 (0.001)
3 ($2\omega_2$)	2.375	2.375 (0.003)	2.375 (0.001)
4 ($\omega_1 + \omega_2$)	2.958	2.959 (0.003)	2.958 (0.002)
5 ($3\omega_2$)	3.060	3.060 (0.004)	3.060 (0.002)
6 ($2\omega_1$)	3.548	3.548 (0.005)	3.548 (0.001)
7 ($2\omega_2 + \omega_1$)	3.635	3.635 (0.008)	3.635 (0.001)

with the DVR benchmark, spanning overtones and combined excitations, but TA SCIVR yields somewhat less precise estimates. This is related to the different widths of the spectral features obtained by means of the two SC approaches. AS SCIVR indeed returns not only accurate but also very precise results due to the small full-width at half maximum (FWHM) values of its signals. FWHM data are definitely larger for TA SCIVR. The better quality of the AS-SCIVR signals is also demonstrated by the fact that well-defined, narrow peaks can be obtained for all 8 eigenvalues employing just the reference state centered at the harmonic ZPE energy. In the case of TA SCIVR if the reference state is not tailored on the state under investigation, then extended bands with several peaks rather than single signals are eventually found for levels 6 and 7. Figure 3 allows to fully appreciate the increased precision of an AS-SCIVR calculation in evaluating the ZPE. In fact, while a very well resolved signal is found for the AS-SCIVR simulation, in the case of TA SCIVR a much larger and asymmetric peak is recovered.

B. H₂O

Water is the first molecule we studied. It is characterized by 3 vibrational degrees of freedom and the well-known Fermi resonance involving the bending overtone and the symmetric stretch. To start with the calculations, we generated AS energy distributions for the ZPE and the energy levels

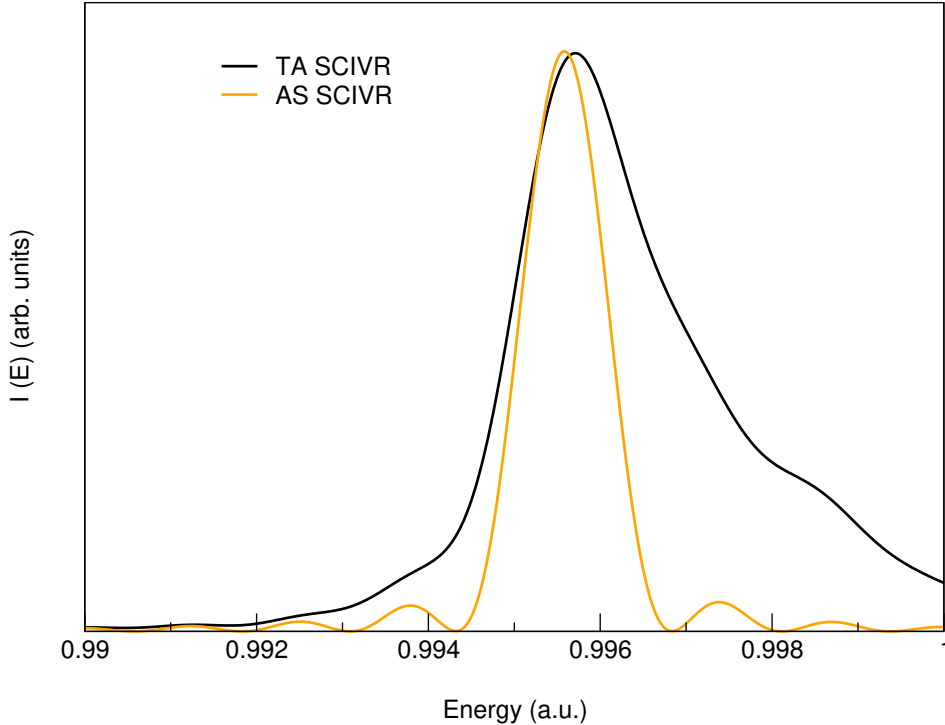


Figure 3. Detail of the ZPE signal for the investigated Henon-Heiles system, as obtained from a standard TA-SCIVR approach (black) and AS SCIVR (orange). Intensities have been scaled to get matching maximum values.

corresponding to the first excitation of the three vibrational modes. Figure 4 shows the similarity of the distributions obtained using either normal mode dynamics or Cartesian dynamics in Eckart frame. We employed the analytical surface by Dressler and Thiel[70]. For the AS procedure we adopted a time step of 10 a.u. for a total T_{AS} time of about 1.2 ps.

For the semiclassical simulations the same time step and total simulation time T were employed. For each AS-SCIVR simulation a distribution of 3 000 initial conditions was obtained upon performing adiabatic switching starting from the harmonic quantization corresponding to the target state, while in the case of the TA-SCIVR calculation a Husimi distribution of 3 000 initial conditions centered at the harmonic ZPE was employed. First, we looked at the fraction of trajectories to be discarded for values of σ ranging from 10^{-2} to 10^{-6} . The TA-SCIVR simulation returned percentages of rejection between 10.1% and 65.4%, while, remarkably, AS SCIVR could

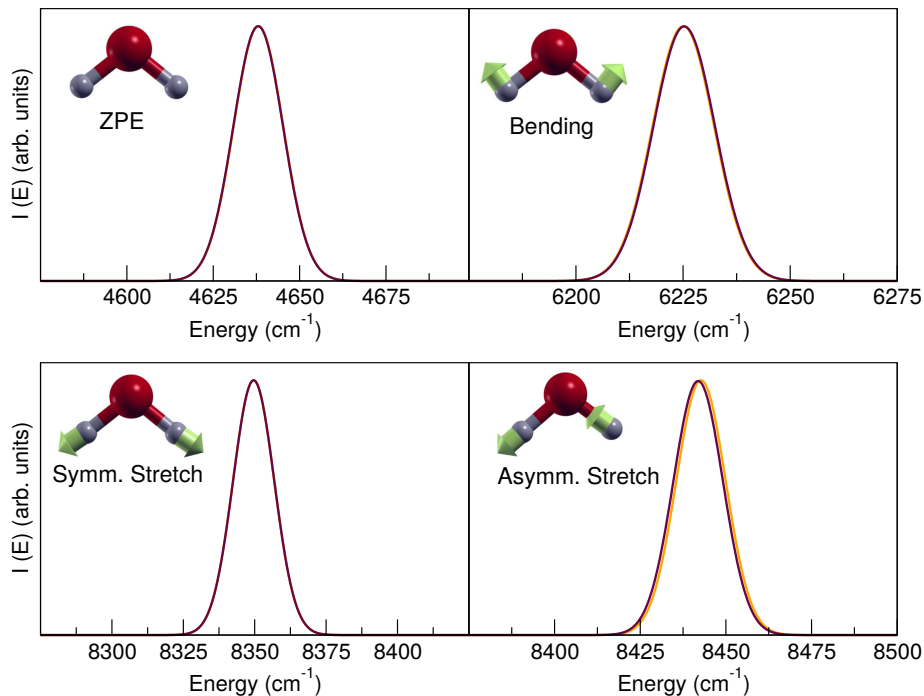


Figure 4. Comparison of adiabatic switching energy distributions for H₂O obtained with Eckart frame Cartesian dynamics (maroon) and normal mode dynamics (orange). The initial harmonic energies are equal to ZPE in panel a); bending excitation in panel b); symmetric stretch excitation in panel c); asymmetric stretch excitation in panel d). The width of the Gaussian envelop of bins was chosen equal to 7.2 cm⁻¹.

rely on the entire set of trajectories independently of the σ threshold.

Moving to the frequencies of vibration, Table II compares the quantum mechanical results obtained by means of a Lanczos algorithm and reported in the Supplementary Information of Ref. 54 to the outcomes of TA SCIVR and the new AS-SCIVR technique. σ was set equal to 10^{-2} , a typical figure we adopt in molecular calculations. Results are slightly better for the AS-SCIVR calculation, whose signals are much more precise as clearly pointed out by the lower FWHM values. However, we notice that most of the error is due to the ZPE estimate. We will discuss more on this point in the final Section of the paper.

Figure 5 presents the power spectra. In particular, from a comparison between the plots reporting the complete spectrum and based on ZPE distributions, it is clear that AS SCIVR gives more precise estimates (this is most evident looking at the symmetric and asymmetric stretches). On the other hand, an AS-SCIVR simulation started from harmonic ZPE quantization yields a harmonic estimate for the overtone, which needs a tailored simulation to be detected correctly.

Table II. ZPE and first vibrational frequencies of H₂O. Frequencies associated to Levels 1-4 are obtained by difference between the corresponding energy level and the ZPE value. Under the Level or Frequency column the harmonic excitation label is given in parenthesis (ω_b for the bending; ω_s for the symmetric stretch; ω_a for the asymmetric stretch). Under the TA SCIVR and AS SCIVR columns, FWHM values are given in parentheses. QM indicates the quantum mechanical benchmark; label HARM is the column of harmonic estimates; MAE stands for mean absolute error. All values are in cm⁻¹.

Level or Frequency	QM ^[54]	TA SCIVR	AS SCIVR	HARM
1 (ω_b)	1587	1590 (42)	1587 (24)	1650
2 ($2 \omega_b$)	3139	3147 (60)	3140 (24)	3300
3 (ω_s)	3716	3711 (41)	3713 (24)	3831
4 (ω_a)	3803	3804 (41)	3808 (24)	3941
ZPE	4660	4642 (34)	4637 (24)	4711
MAE	-	7	6	105

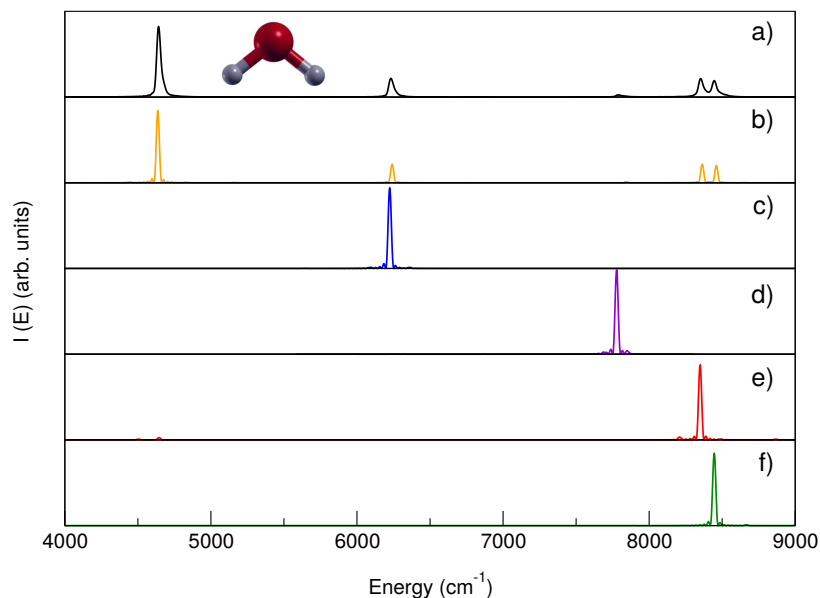


Figure 5. Power spectra of H₂O. Panel a): TA-SCIVR simulation; Panel b): AS-SCIVR simulation from ZPE AS distribution; Panel c) - f): AS-SCIVR simulations from bending, bending overtone, symmetric stretch and asymmetric stretch AS distributions, respectively.

Table III. Percentage of trajectory rejection in TA-SCIVR and AS-SCIVR simulations of H₂CO ($T \approx 0.60$ ps and $T \approx 1.21$ ps) for several rejection thresholds.

σ	$T \approx 0.60$ ps		$T \approx 1.21$ ps	
	TA SCIVR	AS SCIVR	TA SCIVR	AS SCIVR
10^{-2}	47.6%	0.2%	83.5%	22.3%
10^{-3}	56.7%	0.9%	87.2%	38.2%
10^{-4}	65.9%	3.0%	90.9%	57.8%
10^{-5}	75.3%	8.6%	94.0%	77.3%
10^{-6}	84.2%	25.2%	97.0%	93.1%

C. H₂CO

The second molecular system we studied was formaldehyde. We used a pre-existing PES by Martin, Lee, and Taylor.[71] Similarly to the water investigation, for AS we employed a time step of 10 a.u. and a total time T_{AS} of about 1.2 ps. The same values were adopted for TA-SCIVR calculations and the semiclassical part of AS-SCIVR simulations. In all instances a total of 6000 trajectories was run. We do not report AS energy distribution plots for H₂CO but, once more, there is utmost agreement between the normal mode and Cartesian approaches. The threshold for trajectory rejection was set to 10^{-2} . Rejection percentages are reported in Table III, and we notice that, also in this case, AS SCIVR helps a lot in reducing substantially the fraction of discarded trajectories.

Moving to the analysis of the frequencies of vibration, we first focus on fundamentals only. For water and the Henon-Heiles model we performed specific AS-SCIVR calculations for each spectral feature. In the case of H₂CO we wanted to assess the accuracy of a single AS-SCIVR simulation started from harmonic ZPE quantization in estimating the fundamental frequencies. Table IV demonstrates that the numerical outcome is very similar to the TA-SCIVR one.

Differences can be spotted by looking at the corresponding power spectra. Figure 6 reports them. It is clear that the AS-SCIVR procedure provides a better resolution of the spectral signals and helps with the assignment. This is most evident for the band involving the fifth and sixth fundamentals, which TA SCIVR is not able to identify adequately. For this reason, the TA-SCIVR values of ω_5 and ω_6 in Table IV are just tentative and driven by knowledge of the quantum me-

Table IV. Fundamental frequencies of vibration for H_2CO from TA-SCIIVR and AS-SCIIVR simulations based on the harmonic ZPE. Under the Frequency column, the harmonic excitation label is given. QM indicates the quantum mechanical benchmark obtained through a variational approach; label HARM is for the column of harmonic estimates; MAE stands for mean absolute error. FWHM values are given in parentheses. N/A points out that a FWHM value could not be determined. All values are in cm^{-1} .

Frequency	QM ^[72]	TA SCIIVR	AS SCIIVR	HARM
ω_1	1171	1164 (52)	1165 (34)	1192
ω_2	1253	1247 (46)	1247 (34)	1275
ω_3	1509	1509 (48)	1507 (28)	1543
ω_4	1750	1753 (45)	1760 (31)	1781
ω_5	2783	2810 (N/A)	2816 (43)	2929
ω_6	2842	2879 (N/A)	2865 (42)	2996
MAE	-	13	13	68

chanical values. To improve the quality of results, at this point the standard TA-SCIIVR procedure requires additional runs with tailored reference states, but, if more than a single simulation is allowed, then targeted AS-SCIIVR simulations are able to provide more accurate and, most of all, precise estimates, as reported in Table V. For these refined calculations we employed tailored reference states to separate ω_5 and ω_6 in TA-SCIIVR simulations, while we performed 6 different calculations, each one started with one quantum of harmonic excitation in one of the 6 modes, for the AS-SCIIVR case. Tailored TA SCIIVR could resolve between ω_5 and ω_6 , but at the cost of very large peak amplitudes. For refined AS SCIIVR the MAE with respect to the quantum mechanical benchmark, computed on the first 16 frequencies, is down to 8 cm^{-1} .

D. CH_4

The final molecule we present is methane, whose PES and AS energy distribution obtained starting from harmonic ZPE quantization have already been illustrated (see Figures 1 and 2). For this system we decided to perform a single simulation with both AS SCIIVR and TA SCIIVR including all fundamentals, an overtone, and a combined excitation. This allows us to point out the advantages of AS SCIIVR over TA SCIIVR directly.

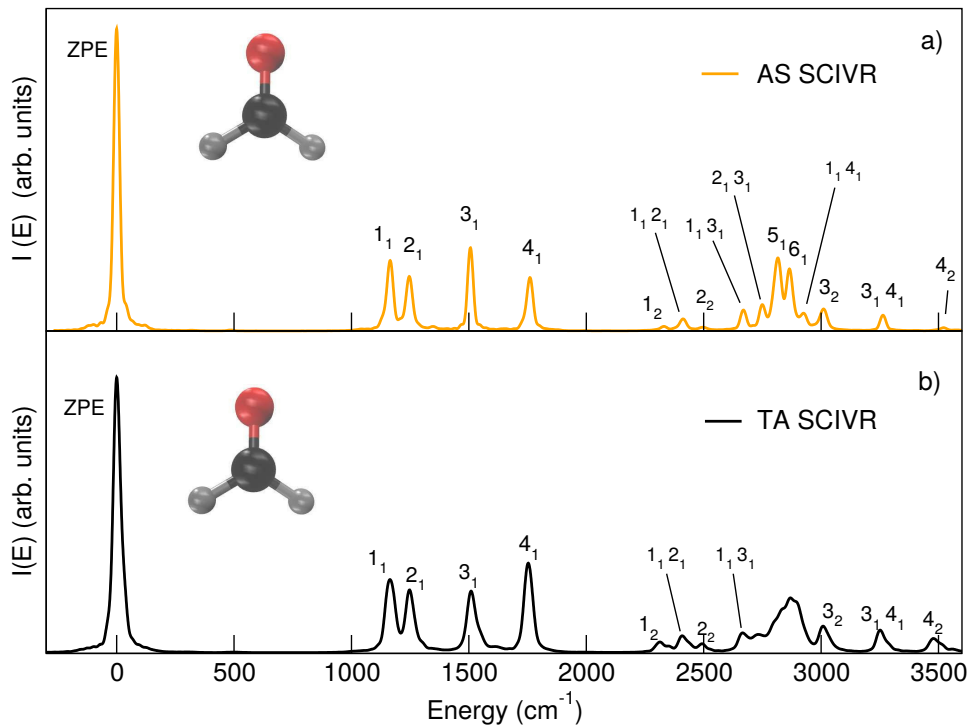


Figure 6. Comparison between AS-SCIIVR (panel a), orange) and TA-SCIIVR (panel b), black) power spectra of formaldehyde.

Table V. TA-SCIIVR and AS-SCIIVR estimates for the first 16 frequencies of vibration for H_2CO . Under the Frequency column, the harmonic excitation label is given. QM indicates the quantum mechanical benchmark; label HARM is for the column of harmonic estimates; MAE stands for mean absolute error. N/A points out that a FWHM value could not be determined. Values are in cm^{-1} .

Frequency	QM ^[72]	TA SCIIVR	AS SCIIVR	HARM	Frequency	QM ^[72]	TA SCIIVR	AS SCIIVR	HARM
ω_1	1171	1164 (52)	1158 (29)	1192	$\omega_2 + \omega_3$	2729	2732 (N/A)	2724 (35)	2818
ω_2	1253	1247 (46)	1245 (30)	1275	ω_5	2783	2813 (98)	2784 (49)	2929
ω_3	1509	1509 (48)	1507 (29)	1543	ω_6	2842	2861 (85)	2844 (33)	2996
ω_4	1750	1753 (45)	1748 (29)	1781	$\omega_1 + \omega_4$	2913	2893 (N/A)	2908 (36)	2973
$2\omega_1$	2333	2313 (78)	2315 (32)	2384	$\omega_2 + \omega_4$	3007	3007 (56)	3009 (37)	3056
$\omega_1 + \omega_2$	2431	2408 (58)	2406 (30)	2467	$2\omega_3$	3016	3007 (56)	3016 (28)	3086
$2\omega_2$	2502	2492 (N/A)	2490 (30)	2550	$\omega_3 + \omega_4$	3250	3252 (48)	3261 (30)	3324
$\omega_1 + \omega_3$	2680	2667 (N/A)	2664 (33)	2735	$2\omega_4$	3480	3478 (67)	3488 (31)	3562
					MAE	-	10	8	64

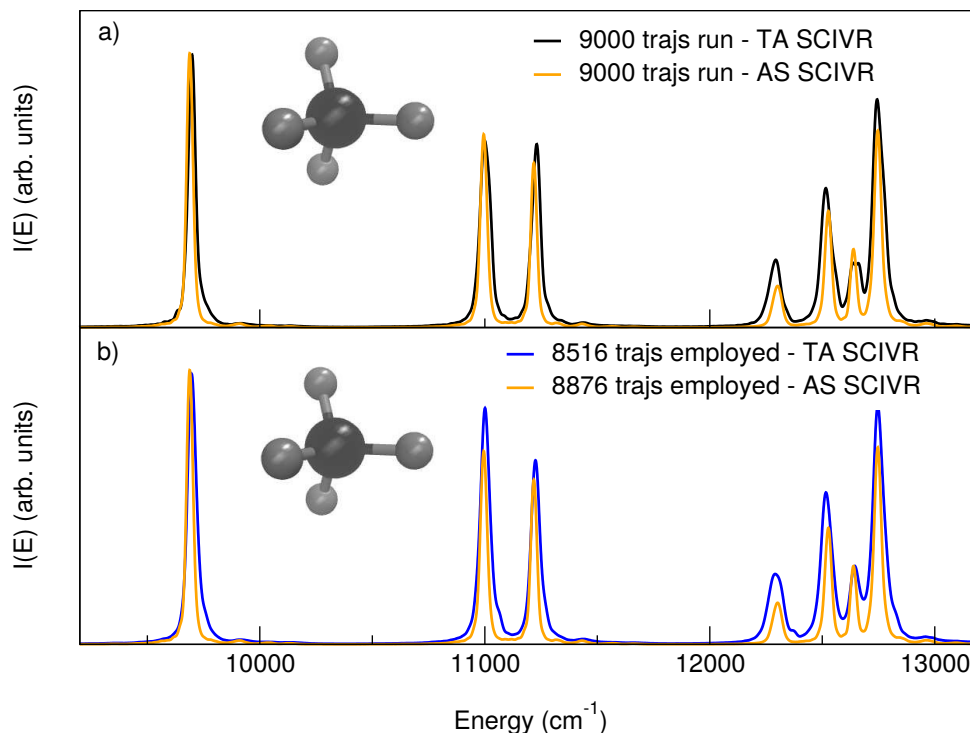


Figure 7. Comparison between methane power spectra obtained from AS-SCIVR (orange) and TA-SCIVR (black/blue) calculations. Panel a): 9 000 trajectories run in both cases. Panel b): Simulations based on similar numbers of non-discarded trajectories. Intensities have been scaled to get matching ZPEs.

Figure 7 is made of two comparisons between AS-SCIVR results obtained starting from harmonic ZPE quantization, and standard TA-SCIVR outcomes collected from a Husimi distribution of initial conditions centered around the harmonic ZPE. We adopted a timestep of 0.242 fs with $T = 1.21$ ps, and a rejection threshold $\sigma = 10^{-2}$. In the first case both simulations were based on 9000 trajectories. While 8876 ($\approx 98.6\%$) of those employed in AS SCIVR were retained for the SC calculation, only 897 trajectories started from the Husimi distribution were kept ($\approx 10\%$). In the second case, we increased to 90 000 the number of trajectories for the TA-SCIVR calculation. In this way 8 516 trajectories were retained to build the TA-SCIVR spectrum, a number comparable to the AS-SCIVR instance. It is clear from Figure 7 that AS SCIVR provides much narrower and more precise signals. However, this is not only due to the higher number of trajectories retained to build the AS-SCIVR spectrum, as the first panel of Figure 7 might suggest, but it is a true hallmark of the method as confirmed by the bottom panel of the same Figure, where the number of trajectories contributing to the spectrum is comparable.

Table VI demonstrates even further the importance of AS SCIVR compared to TA SCIVR in de-

Table VI. Percentage of trajectory rejection in TA-SCIVR and AS-SCIVR simulations of CH₄ ($T \approx 0.60$ ps and $T \approx 1.21$ ps) for several rejection thresholds.

σ	$T = 0.60$ ps		$T = 1.21$ ps	
	TA SCIVR	AS SCIVR	TA SCIVR	AS SCIVR
10^{-2}	54.6%	0.0%	90.4%	1.4%
10^{-3}	61.7%	0.0%	94.0%	5.3%
10^{-4}	70.7%	0.0%	97.3%	16.6%
10^{-5}	81.1%	0.1%	99.0%	42.2%
10^{-6}	90.2%	1.1%	99.7%	79.4%

creasing the number of trajectories displaying a chaotic behavior. As expected, it is also possible to appreciate that numerical stability is worse conserved for higher values of T. Nevertheless, we were able to perform our AS-SCIVR simulations of methane with virtually no trajectory rejection (1.4%). In addition to being more precise, we notice that signals coming from the AS-SCIVR simulation are more accurate when compared to available quantum mechanical results. Table VII points out these aspects, reporting that for AS SCIVR the mean absolute error is down to just 7 wavenumbers with respect to the quantum mechanical benchmark. The investigated methane overtone (level 1.1) and combination excitation (level 1.1 2.1) are basically harmonic at the quantum mechanical level. This has permitted to get excellent AS-SCIVR estimates also for them by means of a single simulation started from harmonic ZPE quantization.

Table VII. Unique frequency values of methane from TA-SCIVR and AS-SCIVR simulations based on a similar number of retained trajectories. Under the Level or Frequency column the harmonic excitation label is given. QM indicates the quantum mechanical benchmark obtained with vibrational self-consistent field theory and a variational approach; label HARM is for the column of harmonic estimates; MAE stands for mean absolute error. FWHM data are reported in parentheses. N/A points out that a FWHM value could not be determined. All values are in cm^{-1} .

Level or Frequency	QM ^[73]	TA SCIVR	AS SCIVR	HARM
ω_1	1313	1305 (51)	1307 (36)	1345
ω_2	1535	1529 (48)	1530 (32)	1570
$2\omega_1$	2624	2594 (80)	2614 (50)	2690
$\omega_1 + \omega_2$	2836	2820 (61)	2839 (36)	2915
ω_3	2949	2948 (N/A)	2950 (34)	3036
ω_4	3053	3050 (58)	3058 (38)	3157
ZPE	9707	9696 (46)	9688 (34)	9842
MAE	-	11	7	77

IV. SUMMARY AND CONCLUSIONS

We have introduced a new strategy, AS SCIVR, to perform quantum vibrational simulations. It is made of a preliminary adiabatic switching procedure for initial conditions followed by a semiclassical spectroscopic calculation. The two main advances introduced by the new technique lie in the very limited number of numerically unstable semiclassical trajectories and the reduced width of spectroscopic signals. Accuracy, which was actually already very good for TA-SCIVR simulations, is also improved, especially when the AS evolution is initiated from the appropriate harmonic quantization. In our AS-SCIVR simulations the mean absolute error with respect to quantum calculations was below 10 cm^{-1} . Furthermore, an AS-SCIVR simulation started from the harmonic ZPE quantization is able to return very good estimates for fundamental frequencies, while it gives a less accurate representation of overtones as it provides merely harmonic values. In these aspects AS SCIVR resembles the MC-SCIVR approach.

While discussing results for H_2O we noticed that it is the ZPE eigenvalue rather than frequency estimates that carries most of the inaccuracy. This is due to the presence of a small amount of

rotational angular momentum in the AS procedure, since molecules are prepared out of equilibrium and normal modes are no longer correctly defined for pure vibrations. We tried to remove the angular momentum before the adiabatic switching dynamics was started obtaining indeed a better ZPE value. For instance, the ZPE of water shifted from 4637 to 4654 cm^{-1} , closer to the quantum mechanical benchmark at 4660 cm^{-1} . However, we found that spectral signals were irregular in shape and much larger, and the technique lost one of its peculiar features making the gain in ZPE accuracy not particularly appealing. Furthermore, frequency values, i.e. the data of interest for comparison to experiments, are calculated by difference between two eigenenergies, so the angular momentum effect cancels out and estimates are accurate. In fact, AS-SCIIVR MAE values, when restricted to fundamentals only, decrease to 3 cm^{-1} for H_2O , and 4 cm^{-1} for CH_4 . An additional confirmation that the angular momentum component is a possible source of inaccuracy in estimating SC eigenvalues comes from our application to the Henon-Heiles model potential. In that case the system was defined in normal modes with no rotation allowed. Remarkably, we were able to reproduce a set of 8 eigenenergies exactly. As for the precision of results, it is known that the presence of rotational angular momentum may affect the width of SC signals. Nagy and Lendvay's internal coordinate adiabatic switching is angular-momentum free and could be helpful, but our approach, which interfaces straightforwardly with the SC calculations, brings in most of the advance overperforming TA SCIIVR neatly and providing very accurate and precise results.

Another important feature of AS SCIIVR is that it can be readily interfaced with any pre-existing semiclassical approach including MC SCIIVR and DC SCIIVR at the affordable cost (with respect to Hessian matrix calculations) cost of just an additional dynamics. This opens up the possibility to achieve a better resolution in simulations involving large dimensional systems, which may help enormously in the difficult assignment of the crowded regions of the spectrum. Furthermore, the diminished probability of trajectory rejection is encouraging, since it increases the probability that in *ab initio* simulations based on a single trajectory the standard prefactor is adopted for the entire dynamics without introduction of any approximation. In fact, rejection is virtually absent (rejection percentage < 5%) in all our AS-SCIIVR calculations, with the exception of H_2CO . Even in this case, though, only at the larger time studied and adopting a very tight threshold, the AS-SCIIVR procedure appears to be less effective. However, these conditions are way too stringent for our *ab initio* on-the-fly simulations, for which we generally employ a threshold $\sigma = 10^{-2}$ and a dynamics about 0.6 ps long.

Finally, in addition to improve SC simulations of large dimensional systems, the AS-SCIIVR

method we have benchmarked in this paper might also serve in perspective as an innovative tool for the semiclassical investigation of floppy systems, which constitute very complex research topics on their own. The initial setup would require a particular care in defining normal modes and the conversion matrix between them and Cartesian coordinates, as largely debated in Ref. 16. Currently the semiclassical study of these systems needs adoption of particular devices mainly consisting in the removal of energy from the large amplitude, low frequency modes.[15, 16] AS SCIVR may help avoid this artefact yielding more accurate and precise frequency estimates.

ACKNOWLEDGMENTS

Authors acknowledge financial support from the European Research Council (Grant Agreement No. (647107)—SEMICOMPLEX—ERC- 2014-CoG) under the European Union’s Horizon 2020 research and innovation programme, and from the Italian Ministry of Education, University, and Research (MIUR) (FARE programme R16KN7XBRB- project QURE). Part of the cpu time was provided by CINECA (Italian Supercomputing Center) under ISCRAB project “QUASP”.

-
- [1] W. H. Miller, *J. Chem. Phys.* **53**, 1949 (1970).
 - [2] E. J. Heller, *Acc. Chem. Res.* **14**, 368 (1981).
 - [3] M. F. Herman and E. Kluk, *Chem. Phys.* **91**, 27 (1984).
 - [4] K. G. Kay, *J. Chem. Phys.* **101**, 2250 (1994).
 - [5] F. Grossmann, *Phys. Rev. A* **60**, 1791 (1999).
 - [6] D. V. Shalashilin and M. S. Child, *J. Chem. Phys.* **115**, 5367 (2001).
 - [7] S. Zhang and E. Pollak, *J. Chem. Phys.* **121**, 3384 (2004).
 - [8] W. H. Miller, *Proc. Natl. Acad. Sci. USA* **102**, 6660 (2005).
 - [9] Y. Zhuang, M. R. Siebert, W. L. Hase, K. G. Kay, and M. Ceotto, *J. Chem. Theory Comput.* **9**, 54 (2012).
 - [10] M. Wehrle, M. Sulc, and J. Vanicek, *J. Chem. Phys.* **140**, 244114 (2014).
 - [11] M. S. Church, S. V. Antipov, and N. Ananth, *J. Chem. Phys.* **146**, 234104 (2017).
 - [12] M. Buchholz, E. Fallacara, F. Gottwald, M. Ceotto, F. Grossmann, and S. D. Ivanov, *Chem. Phys.* **515**, 231 (2018).

- [13] M. S. Church, T. J. Hele, G. S. Ezra, and N. Ananth, *J. Chem. Phys.* **148**, 102326 (2018).
- [14] R. Conte, A. Aspuru-Guzik, and M. Ceotto, *J. Phys. Chem. Lett.* **4**, 3407 (2013).
- [15] G. Di Liberto, R. Conte, and M. Ceotto, *J. Chem. Phys.* **148**, 104302 (2018).
- [16] G. Bertaina, G. Di Liberto, and M. Ceotto, *J. Chem. Phys.* **151**, 114307 (2019).
- [17] M. S. Church and N. Ananth, *J. Chem. Phys.* **151**, 134109 (2019).
- [18] X. Cheng and J. A. Cina, *J. Chem. Phys.* **141**, 034113 (2014).
- [19] M. Buchholz, F. Grossmann, and M. Ceotto, *J. Chem. Phys.* **144**, 094102 (2016).
- [20] F. Gabas, R. Conte, and M. Ceotto, *J. Chem. Theory Comput.* **13**, 2378 (2017).
- [21] F. Gabas, G. Di Liberto, R. Conte, and M. Ceotto, *Chem. Sci.* **9**, 7894 (2018).
- [22] P. A. Kovac and J. A. Cina, *J. Chem. Phys.* **147**, 224112 (2017).
- [23] M. Buchholz, F. Grossmann, and M. Ceotto, *J. Chem. Phys.* **147**, 164110 (2017).
- [24] M. Buchholz, F. Grossmann, and M. Ceotto, *J. Chem. Phys.* **148**, 114107 (2018).
- [25] A. Patoz, T. Begusic, and J. Vanicek, *J. Phys. Chem. Lett.* **9**, 2367 (2018).
- [26] R. Conte, F. Gabas, G. Botti, Y. Zhuang, and M. Ceotto, *J. Chem. Phys.* **150**, 244118 (2019).
- [27] T. Begusic, M. Cordova, and J. Vanicek, *J. Chem. Phys.* **150**, 154117 (2019).
- [28] A. L. Kaledin and W. H. Miller, *J. Chem. Phys.* **118**, 7174 (2003).
- [29] A. L. Kaledin and W. H. Miller, *J. Chem. Phys.* **119**, 3078 (2003).
- [30] E. Kluk, M. F. Herman, and H. L. Davis, *J. Chem. Phys.* **84**, 326 (1986).
- [31] M. Ceotto, Y. Zhuang, and W. L. Hase, *J. Chem. Phys.* **138**, 054116 (2013).
- [32] D. Tamascelli, F. S. Dambrosio, R. Conte, and M. Ceotto, *J. Chem. Phys.* **140**, 174109 (2014).
- [33] X. Ma, G. Di Liberto, R. Conte, W. L. Hase, and M. Ceotto, *J. Chem. Phys.* **149**, 164113 (2018).
- [34] M. Ceotto, G. Di Liberto, and R. Conte, *Phys. Rev. Lett.* **119**, 010401 (2017).
- [35] G. Di Liberto, R. Conte, and M. Ceotto, *J. Chem. Phys.* **148**, 014307 (2018).
- [36] F. Gabas, G. Di Liberto, and M. Ceotto, *J. Chem. Phys.* **150**, 224107 (2019).
- [37] N. De Leon and E. J. Heller, *J. Chem. Phys.* **78**, 4005 (1983).
- [38] M. Ceotto, S. Atahan, G. F. Tantardini, and A. Aspuru-Guzik, *J. Chem. Phys.* **130**, 234113 (2009).
- [39] M. Ceotto, S. Atahan, S. Shim, G. F. Tantardini, and A. Aspuru-Guzik, *Phys. Chem. Chem. Phys.* **11**, 3861 (2009).
- [40] M. Ceotto, G. F. Tantardini, and A. Aspuru-Guzik, *J. Chem. Phys.* **135**, 214108 (2011).
- [41] M. Ceotto, S. Valleau, G. F. Tantardini, and A. Aspuru-Guzik, *J. Chem. Phys.* **134**, 234103 (2011).
- [42] L. D. Landau and E. M. Lifshitz, *Mechanics* (Elsevier, 1982).

- [43] E. A. Solovev, Zh. Eksp. Teor. Fiz. **75**, 1261 (1978).
- [44] R. T. Skodje, F. Borondo, and W. P. Reinhardt, J. Chem. Phys. **82**, 4611 (1985).
- [45] B. R. Johnson, J. Chem. Phys. **83**, 1204 (1985).
- [46] S. Saini, J. Zakrzewski, and H. S. Taylor, Phys. Rev. A **38**, 3900 (1988).
- [47] J. Huang, J. J. Valentini, and J. T. Muckerman, J. Chem. Phys. **102**, 5695 (1995).
- [48] A. Bose and N. Makri, J. Chem. Phys. **143**, 114114 (2015).
- [49] A. Bose and N. Makri, J. Chem. Theory Comput. **14**, 5446 (2018).
- [50] B. R. Johnson, J. Chem. Phys. **86**, 1445 (1987).
- [51] Q. Sun, J. M. Bowman, and B. Gazdy, J. Chem. Phys. **89**, 3124 (1988).
- [52] C. Qu and J. M. Bowman, J. Phys. Chem. A **120**, 4988 (2016).
- [53] T. Nagy and G. Lendvay, J. Phys. Chem. Lett. **8**, 4621 (2017).
- [54] M. Micciarelli, R. Conte, J. Suarez, and M. Ceotto, J. Chem. Phys. **149**, 064115 (2018).
- [55] M. Micciarelli, F. Gabas, R. Conte, and M. Ceotto, J. Chem. Phys. **150**, 184113 (2019).
- [56] C. Aieta, F. Gabas, and M. Ceotto, J. Phys. Chem. A **120**, 4853 (2016).
- [57] C. Aieta, F. Gabas, and M. Ceotto, J. Chem. Theory Comput. **15**, 2142 (2019).
- [58] R. Conte and M. Ceotto, *Semiclassical Molecular Dynamics for Spectroscopic Calculations* (Wiley, book chapter, accepted).
- [59] K. G. Kay, J. Chem. Phys. **100**, 4432 (1994).
- [60] V. Guallar, V. S. Batista, and W. H. Miller, J. Chem. Phys. **110**, 9922 (1999).
- [61] R. Gelabert, X. Giménez, M. Thoss, H. Wang, and W. H. Miller, J. Phys. Chem. A **104**, 10321 (2000).
- [62] G. Di Liberto and M. Ceotto, J. Chem. Phys. **145**, 144107 (2016).
- [63] J. Tatchen, E. Pollak, G. Tao, and W. H. Miller, J. Chem. Phys. **134**, 134104 (2011).
- [64] T. J. Lee, J. M. Martin, and P. R. Taylor, J. Chem. Phys. **102**, 254 (1995).
- [65] M. L. Brewer, J. S. Hulme, and D. E. Manolopoulos, J. Chem. Phys. **106**, 4832 (1997).
- [66] H. Wang, D. E. Manolopoulos, and W. H. Miller, J. Chem. Phys. **115**, 6317 (2001).
- [67] D. Huber and E. J. Heller, J. Chem. Phys. **89**, 4752 (1988).
- [68] D. Huber, S. Ling, D. G. Imre, and E. J. Heller, J. Chem. Phys. **90**, 7317 (1989).
- [69] D. T. Colbert and W. H. Miller, J. Chem. Phys. **96**, 1982 (1992).
- [70] S. Dressler and W. Thiel, Chem. Phys. Lett. **273**, 71 (1997).
- [71] J. Martin, T. J. Lee, and P. Taylor, J. Mol. Spectr. **160**, 105 (1993).
- [72] S. Carter, N. Pinnavaia, and N. C. Handy, Chem. Phys. Lett. **240**, 400 (1995).

[73] S. Carter, H. M. Shnider, and J. M. Bowman, *J. Chem. Phys.* **110**, 8417 (1999).